

# Eliminating irreproducibility in SERS substrates

David-Benjamin Gry's<sup>1</sup> | Rohit Chikkaraddy<sup>1</sup> | Marlous Kamp<sup>1</sup> |  
 Oren A. Scherman<sup>2</sup> | Jeremy J. Baumberg<sup>1</sup> | Bart de Nijs<sup>1</sup>

<sup>1</sup>Nanophotonics Centre, Department of Physics, University of Cambridge, Cambridge, UK

<sup>2</sup>Melville Laboratory for Polymer Synthesis, Department of Chemistry, University of Cambridge, Cambridge, UK

## Correspondence

Jeremy J. Baumberg and Bart de Nijs,  
 Nanophotonics Centre, Department of Physics, University of Cambridge,  
 Cambridge CB3 0HE, UK.  
 Email: jjb12@cam.ac.uk;  
 bd355@cam.ac.uk

## Funding information

EPSRC, Grant/Award Numbers: EP/L027151/1, EP/P029426/1, EP/R020965/1; Trinity College, University of Cambridge; EPSRC Centre for Doctoral Training in Sensor Technologies and Applications, Grant/Award Number: EP/L015889/1; Winton Programme for the Physics of Sustainability; Leverhulme Trust, Grant/Award Number: ECF; Isaac Newton Trust

## Abstract

Irreproducibility in surface-enhanced Raman spectroscopy (SERS) due to variability among substrates is a source of recurrent debate within the field. It is regarded as a major hurdle towards the widespread adoption of SERS as a sensing platform. Most of the literature focused on developing substrates for various applications considers reproducibility of lower importance. Here, we address and analyse the sources of this irreproducibility in order to show how these can be minimised. We apply our findings to a simple substrate demonstrating reproducible SERS measurements with relative standard deviations well below 1% between different batches and days. Identifying the sources of irreproducibility and understanding how to reduce these can aid in the transition of SERS from the lab to real-world applications.

## KEY WORDS

cucurbituril, repeatability, reproducibility, self-assembly, SERS | plasmonics

## 1 | INTRODUCTION

The extreme sensitivity of surface-enhanced Raman spectroscopy (SERS) makes this technique a promising and powerful sensing platform.<sup>[1]</sup> With hardware components such as lasers and detectors rapidly reducing in cost, SERS has the potential to become an economically viable technique<sup>[2]</sup> with broad adoption in medical diagnosis,<sup>[2]</sup> environmental monitoring,<sup>[3]</sup> drug detection,<sup>[4]</sup> food quality control<sup>[5–10]</sup> and continuous health screening.<sup>[11]</sup>

As first identified by Jeanmaire and van Duyne in 1977, this extraordinary sensitivity stems from the powerful field enhancements that can arise in nanostructured

metal surfaces.<sup>[12]</sup> Since then, an impressive volume of literature has emerged around the subject with a wide range of different methods employed to achieve field enhancements.<sup>[13–15]</sup> Unfortunately, the source of this high sensitivity is also the predominant cause for poor reproducibility. As the SERS enhancement scales with  $|E/E_0|^4$ , small changes in the in- and out-coupling or perturbations in near-field enhancement ( $E/E_0$ ) drastically alter SERS intensities.<sup>[16]</sup> Even gold atom migration plays a role in the reproducibility and performance of such SERS substrates.<sup>[17]</sup> It is therefore essential to have nanometre-scale, and preferably even atomic-scale, control over the substrate.

This is an open access article under the terms of the Creative Commons Attribution License, which permits use, distribution and reproduction in any medium, provided the original work is properly cited.

© 2020 The Authors. Journal of Raman Spectroscopy published by John Wiley & Sons Ltd

The vast body of work on SERS sensing predominately focuses on developing substrates or identifying new applications. Authors frequently report on a sensor's performance in terms of repeatability and reproducibility, but this is often regarded as secondary to other quantities such as detection limit and signal strength. Despite the lack of a standardised figure of merit for quantifying variance in SERS substrates,<sup>[18]</sup> the most widely encountered metric in the literature is the relative standard deviation (RSD). It is calculated by normalising the standard deviation of a vibrational peak intensity by its mean value. A well-performing substrate exhibits RSD values between 5% and 15%, but RSDs exceeding 15% are often still considered to be a 'good' result.

Here, we demonstrate that for a simple SERS substrate based on aqueous suspensions of gold nanoparticle (AuNP) aggregates, it is possible to nearly eliminate

variance (RSDs below <1%) if parameters such as interparticle spacing and aggregation time are controlled. This allows us to study environmental and timing factors applicable to other SERS substrates. The key ingredient for achieving this high reproducibility is a molecular linker (cucurbit[n]uril: CB[n]<sup>[19]</sup>) that binds AuNPs with fixed interparticle spacing (Figure 1a). The self-assembly of the substrate is initiated by mixing a CB[n] solution with citrate-stabilised AuNPs using a micropipette in, for example, a multiwell plate. This one-step protocol greatly increases reproducibility compared with more complex top-down fabrication requiring multiple sample preparation steps. In addition, with both standardised AuNPs and CB[n] now commercially available at affordable prices, such substrates are readily accessible for anyone to employ provided they quantify these RSDs.

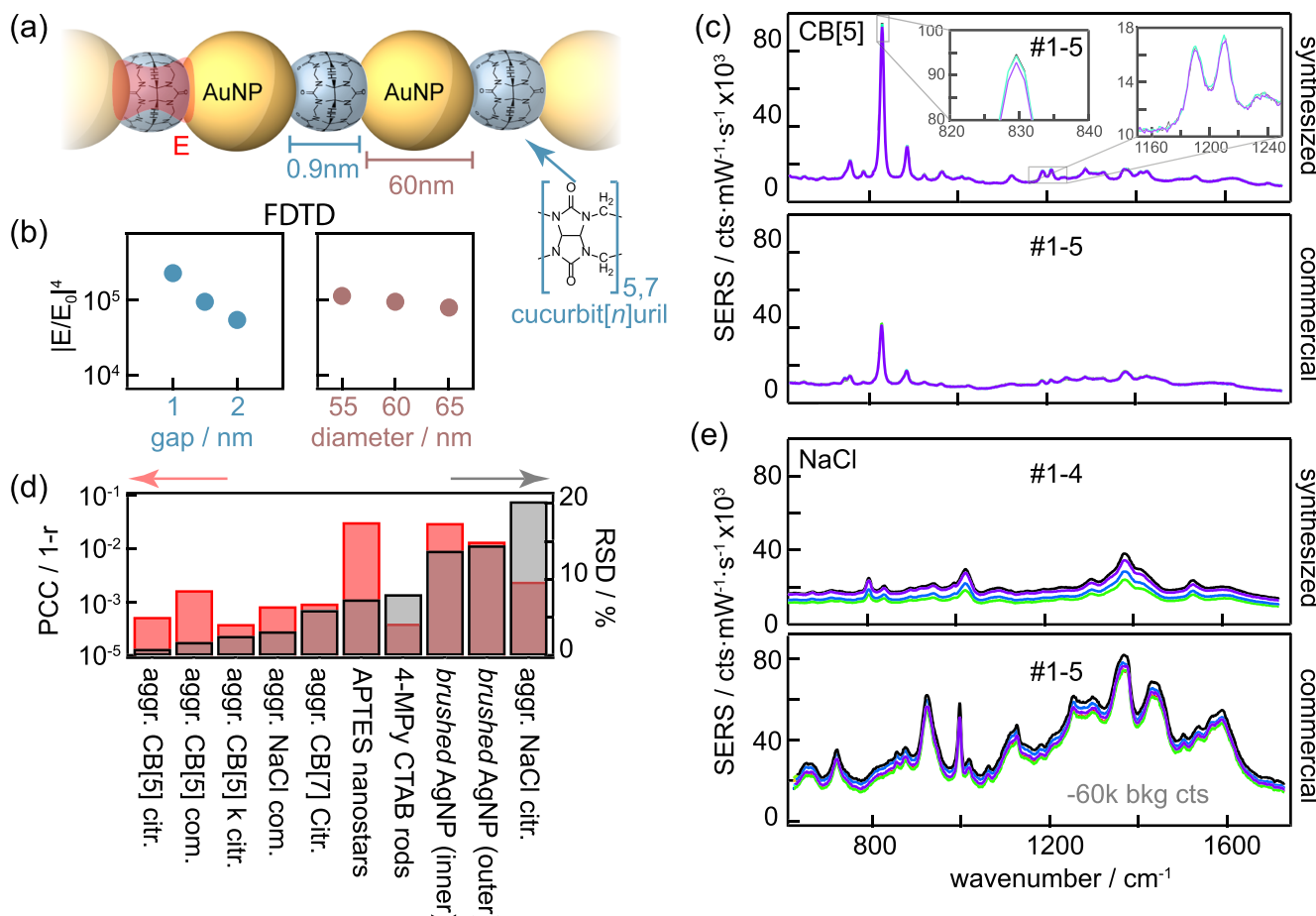


**FIGURE 1** Reproducibility in surface-enhanced Raman spectroscopy (SERS) substrates. (a) Schematic representation of CB[5]-aggregated AuNPs with 0.9 nm separation. (b) FDTD simulation of SERS enhancement as a function of gap size and AuNP size (calculated as  $E^2_{633\text{nm}} \times E^2_{700\text{nm}}$ ). (c) SERS spectra comparison between homemade (top) versus commercial (bottom) AuNPs aggregated using CB[5], showing comparable reproducibility but lower counts for commercial AuNPs. Each spectrum represents another batch taken on a different day. (d) Comparison of the reproducibility for various SERS substrates using a Pearson correlation coefficient analysis and the relative standard deviation (RSD). (e) Salt-induced aggregation of both types of AuNP, showing larger spectral variance and an increased background for commercial particles

## 2 | MATERIALS AND METHODS

### 2.1 | Nanoparticles

Commercial AuNPs with 60 nm average diameter in sodium citrate buffer are purchased from BBI Solutions. To compare variances stemming from undisclosed surfactants and chemical residues of the commercial product, in-house AuNPs are synthesised according to the standard method published by Turkevich et al.<sup>[20]</sup> and Frens.<sup>[21]</sup> To create AuNPs with an average diameter of ~60 nm, a citrate to HAuCl<sub>4</sub> ratio of 1.33 is chosen. The synthesis is performed both with tri-sodium citrate (Na<sub>3</sub>citrate) and with tri-potassium citrate (K<sub>3</sub>citrate) to explore the effects of counterions on reproducibility. All chemicals are purchased from Sigma-Aldrich and used as received.

### 2.2 | SERS measurement protocol

All experiments are performed using black polypropylene 96 multiwell plates with a well volume of 340 µl, as cross-linked polystyrene multiwell plates (often used in biological applications) are found to leak contaminants, likely resulting from a lower chemical resistance to acetone, one of the major thermal breakdown products of AuNP suspensions. Dissolved polystyrene is found to interfere with aggregation kinetics and to infiltrate plasmonic hot-spots where it occupies binding sites, contaminating the SERS signals due to its large Raman cross section, with peaks at 1000, 1030 and 1600 cm<sup>-1</sup>.

In a typical experiment to prepare cucurbit[n]uril (CB[n]):AuNP aggregates, 333 µl colloidal AuNP suspension is added to 7 µl of a 15.6 µM CB[n] solution using Eppendorf Research Plus single channel micropipettes of 1 ml and 10 µl, respectively. As this nanoassembly exhibits a very low detection limit (nanomolar range), it is essential to keep pipettes clean and free of contaminants. Unless otherwise stated, the solution/suspension is allowed to aggregate for exactly 10 min ( $\pm 5$  s) before a SERS spectrum is taken. The aggregation time is measured and checked with a digital timer.

For experiments involving methyl viologen (MV<sup>2+</sup>), the protocol above is amended by pipetting only 293 µl of the AuNP suspension and adding 40 µl of a MV<sup>2+</sup> solution with concentrations ranging from 7.8·10<sup>-4</sup> to 1·10<sup>-8</sup> M using a 100 µl Eppendorf pipette of the same make. Because different aggregation and incubation times are analysed, the exact times for CB[n]:AuNP:MV<sup>2+</sup> measurements are stated in the text. The aggregation and incubation times are measured from the moment of mixing. Salt-mediated aggregation is

performed with 40 µl of a 0.5M NaCl stock solution followed by 300 µl of the AuNP suspension. Again, the aggregation time is precisely fixed to 10 min ( $\pm 5$  s). It is important to stress that each measurement is carried out using a freshly prepared sample, strictly adhering to the stated aggregation and incubation times.

After the aggregation (or in case of MV<sup>2+</sup>, incubation) time has passed, three consecutive spectra with 10s exposure are immediately taken and averaged. Spectra are collected with a Renishaw InVia Raman system using the same 5× objective for each measurement. The 785 nm laser is given sufficient time to warm up and delivers 130 ± 1 mW laser power onto the sample. Before each set of measurements, the Raman shift is calibrated to a silicon reference. To ensure consistency, the focal plane is set near the liquid/air interface optimised to the highest CB[5]:AuNP signal counts (within  $\pm 75$  µm in height). In order to make the measured intensities of SERS spectra more comparable between different publications, our reported results are all normalised to the product of laser power (mW) and exposure time (s).

## 3 | RESULTS AND DISCUSSION

Forming nanogaps between plasmonic nanoparticles is the most common bottom-up colloidal method for achieving SERS enhancement.<sup>[22]</sup> Nanogaps provide high enhancement but are also extraordinarily sensitive to even slight variations in size.<sup>[23,24]</sup> Increasing a 1 nm gap by just 1.7 Å (the radius of one gold atom) affects the field enhancement more than varying the diameter of 60 nm AuNPs by 10 nm (Figure 1b). This potential source of variance can be avoided by using a molecular spacer such as CB[n], which binds AuNPs with a fixed interparticle spacing of 0.9 nm<sup>[25]</sup> (Figure 1a).

Controlling the time between the start of aggregation and acquisition is essential to obtain reproducible spectra because the self-assembly of CB[n]:AuNPs aggregates is a time-varying process. After 10min ( $\pm 5$  s) aggregation time, the superposition of five unique CB[5]:AuNP spectra taken on different days (different batches) is almost perfectly congruent, showing the CB[5] vibrational spectrum (Figure 1c). This means that both background and spectral shape are nearly identical, with an RSD of 0.8% (Figure 1d). Here, the CB[5] concentration (312 nM) is optimised to maximise the signal counts, which increases the RSD value. For higher CB[5] concentrations, the signal variance is consistently low.

Another important factor that determines the long-term reproducibility is a consistent surface chemistry of the AuNPs used. Comparing our synthesised (Figure 1c, top) to commercial (Figure 1c, bottom) AuNPs shows a

45% drop in signal intensity resulting in a poorer RSD of 1.7%. This difference in CB[5] binding between commercial and synthesised AuNPs is the result of different surface chemistries, as supported by the disagreeing SERS fingerprints obtained through NaCl salting (Figure 1e, top and bottom). Instead, in-house AuNPs are fully citrate-stabilised ( $\text{pH} = 3.5 \pm 0.1$ ) and synthesised without the addition of any other surfactant. The commercial AuNPs, though citrate-buffered at a higher pH ( $6.8 \pm 0.2$ ), likely contain additional surfactants and/or chemical residues from their synthesis. As the synthesis protocol is not disclosed by the manufacturer, we cannot report on the chemical composition.

As an alternative to RSDs, we introduce the Pearson correlation coefficient  $r$  (PCC, plotted in Figure 1d as  $1 - r$  on a log scale), which is more suitable for characterising variance due to chemical inconsistencies; PCC measures the similarity in shape between pairs of SERS spectra whilst ignoring the background shifts often encountered in SERS spectra. This can be seen for the salt-induced aggregation (Figure 1e, top and bottom), which yields comparably high PCCs (similar shape) despite the clearly noticeable background fluctuations.

The highest PCCs were found for our synthesised AuNPs aggregated using CB[5], yielding PCCs of  $R = 0.9994$  ( $\text{Na}_3\text{citrate}$ ), 0.9996 ( $\text{K}_3\text{citrate}$ ) and 0.9983 (commercial). Interestingly, using  $\text{K}_3\text{citrate}$ -stabilised instead of  $\text{Na}_3\text{citrate}$ -stabilised AuNPs yields a 30% improved PCC but also slightly increases the RSD. Both AuNPs are synthesised using the same protocol resulting in the same size distribution. This shows that the choice of counterions can play a role in the reproducibility of SERS substrates. Moreover, exchanging CB[5] for its larger homologue CB[7] has little effect on the PCC, but significantly increases the RSD (5.9%). As the larger CB[7] is less rigid and also more prone to sequestering molecules in its hydrophobic gap, this can alter the dielectric constant of the gap<sup>[26]</sup> and might also interfere with the vibrational spectra of CB[7] itself.<sup>[27]</sup>

Similarly high PCCs (0.9996) are achieved in the work by Bi et al. where CTAB, 4-mercaptopuridine (4-MPY) nanorods are self-assembled into tightly packed arrays.<sup>[28]</sup> The rigid ligands together with the ordered structure provide consistent spacing and controlled hotspot intensities, resulting in highly reproducible signals. This good reproducibility comes at the expense of complexity as this work involves careful colloidal synthesis and self-assembly. In contrast, Zhang et al.<sup>[29]</sup> demonstrate how an effective SERS substrate can be formed by simply brushing AgNPs on microfluidic paper, but, as expected, this in turn comes at the cost of reproducibility, which is reflected in both the degraded PCCs and RSDs.

Apart from SERS substrates based on plasmonic enhancement from nanogaps, sharp features through top-down fabrication or colloidal synthesis can also provide considerable field enhancement and low RSDs. APTES-functionalised nanostars, as reported by Su et al.,<sup>[30]</sup> give RSDs of ~7% in spite of having a lower PCC compared with salt-aggregated AuNPs. Such nanostars do not require any self-assembly step as their shape yields sufficient field enhancements. They can readily be synthesised in bulk, or potentially even in flow reactors. However, nanostars deposited on surfaces tend to aggregate and sinter, which then leads to a second source of field enhancements (nanogaps), negatively affecting reproducibility.<sup>[30]</sup>

To put these RSDs into context, a range of RSD values reported in the literature is compiled in Figure 2a (labelled as **1–49**). From this, it is clear that RSDs generally vary anywhere between 5% and 25%, with a wide range of materials and nanostructures used. Notably, for the two non-aggregate SERS substrates in the top 5 (**3, 5**), the authors take special care to control the nanogap spacings reporting RSDs below 3%. To this end, the authors either employ an ultrathin aluminium mask (**3**) that sets the spacing<sup>[31]</sup> or combine deep UV with large nanogaps ( $30 \pm 5$  nm) (**5**), placing them in a less sensitive distance dependent regime.<sup>[32]</sup> Using nanostars can circumvent the need for nanogaps but in turn suffers from the need to carefully control the nanostar shape. Although single batch substrates can generate highly repeatable spectra, it is difficult to synthesise nanostars with precisely similar sharp point geometries, negatively affecting batch to batch reproducibility.

In general, there is a tendency to report on repeatability instead of reproducibility for SERS substrates based on more complex fabrication methods. Repeatability is a weaker measure of variance, often calculated by taking the RSD values between multiple measurement points from a single substrate,<sup>[18]</sup> indicated in Figure 2a with a blue outline. Considering only RSD reported for reproducibility, aggregate-based nanoassemblies (blue filled bars in Figure 2a) appear to provide both the best and worst reproducibility, topped by CB[5]:AuNP aggregates with an RSD of 0.8%. For such aggregates to generate repeatable spectra, a homogeneous distribution of aggregates is essential. In substrates (**1**), (**2**), (**4**), (**6**), (**8**), (**9**), (**13**), (**14**), and (**15**), this is achieved by keeping aggregates in suspension, whereas in (**7**), a hydrophobic surface is employed forcing dense homogeneous packing of aggregates. From this overview, it is also evident that gold yields better RSDs over silver. This is attributed to the formation of oxide layers reducing signal strengths,<sup>[66]</sup> thus affecting reproducibility. Whilst gold is more expensive than silver,

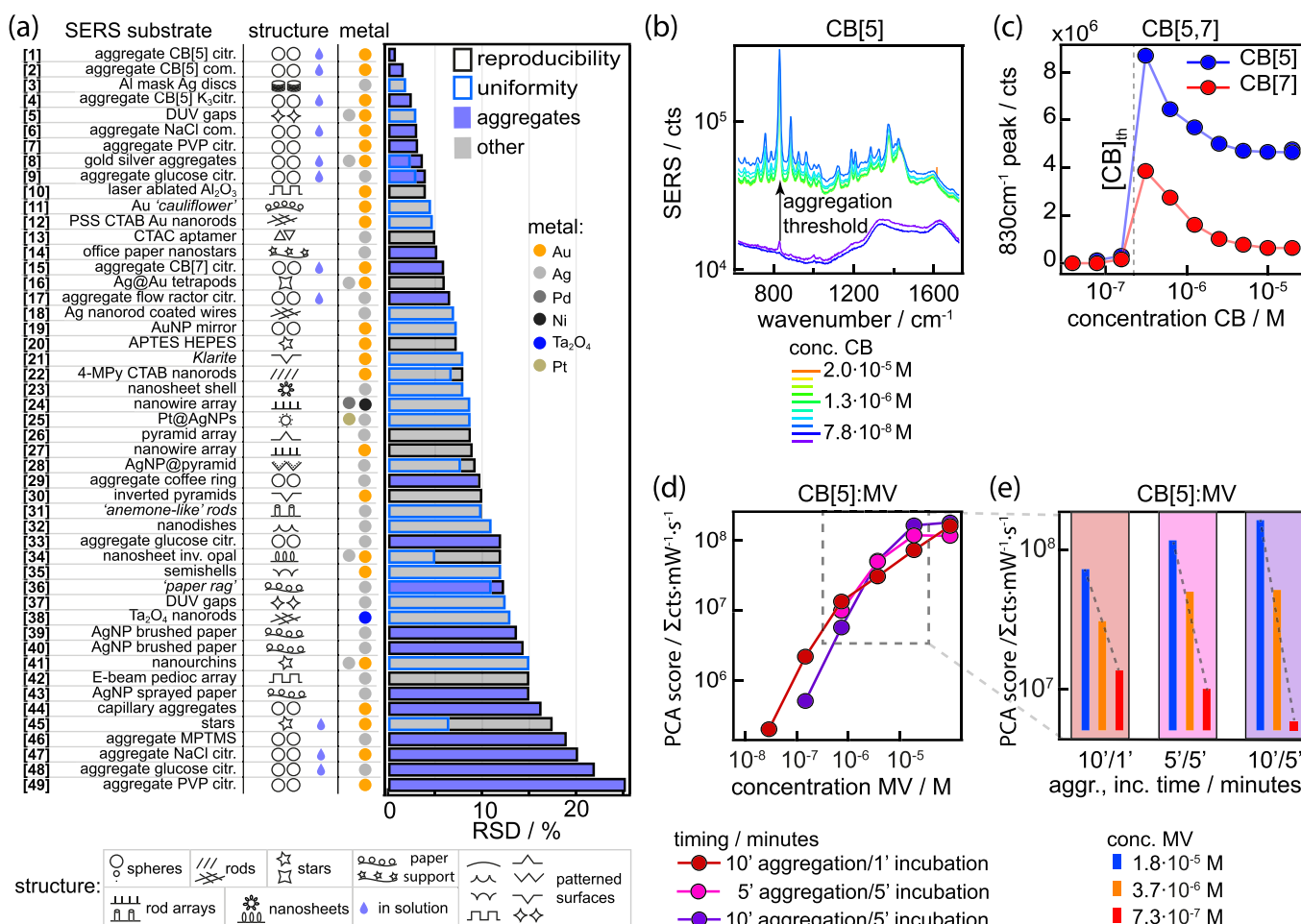


**FIGURE 2** Factors influencing relative standard deviations (RSDs) in surface-enhanced Raman spectroscopy (SERS). (a) Comparison between RSDs from various SERS substrates as reported in literature or presented in this work. Values are collated from the following literature: 3,<sup>[31]</sup> 5,<sup>[32]</sup> 7,<sup>[33]</sup> 8,<sup>[34]</sup> 9,<sup>[35]</sup> 10,<sup>[36]</sup> 11,<sup>[37]</sup> 12,<sup>[38]</sup> 13,<sup>[39]</sup> 14,<sup>[40]</sup> 16,<sup>[41]</sup> 17,<sup>[42]</sup> 18,<sup>[43]</sup> 19,<sup>[44]</sup> 20,<sup>[30]</sup> 21,<sup>[32]</sup> 22,<sup>[28]</sup> 23,<sup>[45]</sup> 24,<sup>[46]</sup> 25,<sup>[47]</sup> 26,<sup>[48]</sup> 27,<sup>[49]</sup> 28,<sup>[50]</sup> 29,<sup>[51]</sup> 30,<sup>[52]</sup> 31,<sup>[53]</sup> 32,<sup>[54]</sup> 33,<sup>[55]</sup> 34,<sup>[56]</sup> 35,<sup>[57]</sup> 36,<sup>[58]</sup> 37,<sup>[32]</sup> 38,<sup>[59]</sup> 39,<sup>[29]</sup> 40,<sup>[29]</sup> 41,<sup>[60]</sup> 42,<sup>[61]</sup> 43,<sup>[62]</sup> 44,<sup>[63]</sup> 45,<sup>[64]</sup> 46,<sup>[65]</sup> 48,<sup>[55]</sup> 49.<sup>[33]</sup> (b) SERS signal for CB[5,7] aggregates for different CB concentrations. (c) Extracted peak intensity plotted against CB concentration, showing signal increase with reduced concentration. (d) PCA scores of methyl viologen concentration series for different aggregation and incubation times. (e) Extracted PCA scores demonstrating how variations arising from aggregation and incubation influence dynamic range

the gain in reproducibility outweighs the increased base material cost.

The lowest RSD value (**1**) is the result of careful optimisation with the goal of controlling variance in the system whilst maximising signal intensity. Even though CB[5] forms precise nanogaps, the morphology of the aggregates plays an important role in SERS enhancement. The enhancement factor and light coupling depend on the average chain length and shape of the aggregates, which grow as the aggregation proceeds. Hence, the aggregation time must be precisely controlled to remove this source of variance, keeping relative concentrations constant. A CB concentration series (Figure 2b,c) shows that the largest enhancement is achieved close to the aggregation threshold (i.e., the CB[n] concentration that just induces AuNP aggregation) where the aggregates have the most

efficient morphology for SERS. Such aggregates exhibit an open fractal-like structure as a result of diffusion-limited aggregation.<sup>[25]</sup> However, at this point, slight concentration variations (e.g., through inaccurate pipetting) can lead to a different aggregate shape and thus reduced repeatability.

In a similar fashion to the aggregation process, the incubation time also requires careful control when introducing an analyte to the SERS substrate, because equilibration between the analyte in solution and the plasmonic hotspots requires time. A concentration series of MV<sup>2+</sup> added to the CB[5]/AuNP aggregates at different aggregation versus incubation times (Figure 2d) reveals large fluctuations in signal strength. Choosing both a long aggregation and incubation time (10:5 min) results in very large aggregates that begin to precipitate out of

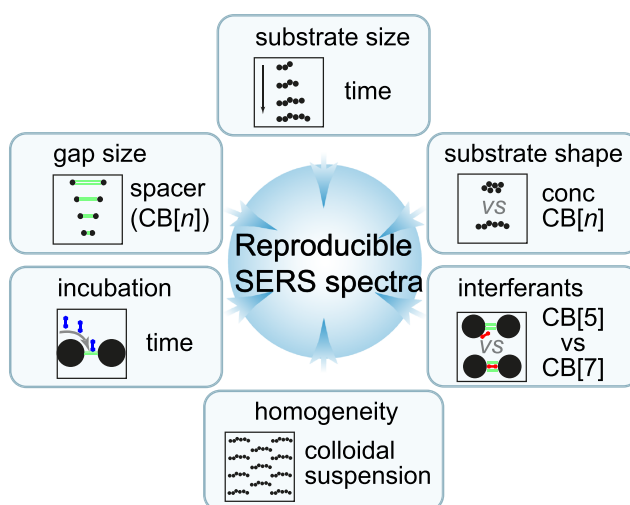


**FIGURE 3** Overview of factors identified influencing reproducibility in surface-enhanced Raman spectroscopy spectra and how they are addressed in this work to yield relative standard deviations  $< 1\%$

the solution. This effectively reduces the detection limit for low  $MV^{2+}$  concentrations compared with a shorter incubation time (10:1 min). Similarly, a high  $MV^{2+}$  concentration implies a high AuNP surface coverage, which stabilises the aggregates by preventing further growth. Depending on the application, it is thus possible to shift the dynamic range so that a specific sensitivity and concentration range is attained (Figure 2e). This shows that understanding and carefully controlling parameters (which appear to be weaknesses) instead can be turned into useful features.

It is important to note that when using aggregation to form SERS substrates, analytes and interferants can alter the aggregation process. This means that aggregates need to be formed in a chemically controlled environment *prior* to combining with an analyte solution to ensure reproducibility. This will become even more important when probing real-world samples as ion concentrations will vary and unknown organic moieties will be present.

As shown here, SERS can be sensitive and highly reproducible at the same time. However, this requires control of all parameters because every step in the process from manufacturing/self-assembly to incubation and measurement will affect the reproducibility. All parameters identified in this work are collated in Figure 3.

## 4 | CONCLUSION

We presented a systematic analysis with the goal to identify various sources of variance, which in general affect

the reproducibility of SERS substrates. When applying these findings to our simple prototypical substrate, we achieve highly reproducible SERS spectra with RSDs below 1%.

For the self-assembled  $CB[n]/AuNPs$  aggregates with their precisely defined nanogaps, we find that reproducibility is eventually determined by environmental factors such as accurate timings for aggregation and analyte incubation. Moreover, we compared the  $CB[n]/AuNPs$  substrate to various approaches found in the literature and discussed their sources of variance.

Because the degree of control has to be very tight to reach a reproducibility as high as presented here, automation can likely play a major role in ensuring accurate timings and dispensed volumes. Via this route, we believe that it will be possible to acquire sufficiently large datasets for quantitative sensing.

## ACKNOWLEDGEMENTS

We gratefully acknowledge Dr Qianqian Su, Professor Lingxin, Dr Bowei Li and Dr Liyan Bi for generously providing the original SERS data used for their research, to be used for the Pearson correlation analysis. We acknowledge financial support from the EPSRC EP/L027151/1, EP/P029426/1 and EP/R020965/1. R. C. acknowledges support from Trinity College, University of Cambridge. BdN acknowledges financial support from the Leverhulme Trust and the Isaac Newton Trust in the form of an ECF, BdN and MK acknowledge support from the Winton Programme for the Physics of Sustainability, and DBG acknowledges support from the EPSRC Centre for Doctoral Training in Sensor Technologies and Applications (EP/L015889/1).

## CONFLICT OF INTEREST

The Authors declare no competing financial interests.

## SUPPORTING INFORMATION

The data supporting the findings of this study are openly available at <https://doi.org/10.17863/CAM.58235>.

## ORCID

David-Benjamin Grys  <https://orcid.org/0000-0002-4038-6388>

Rohit Chikkaraddy  <https://orcid.org/0000-0002-3840-4188>

Marlous Kamp  <https://orcid.org/0000-0003-4915-1312>

Oren A. Scherman  <https://orcid.org/0000-0001-8032-7166>

Jeremy J. Baumberg  <https://orcid.org/0000-0002-9606-9488>

Bart de Nijs  <https://orcid.org/0000-0002-8234-723X>

## REFERENCES

- [1] C. L. Haynes, A. D. McFarland, R. P. Van Duyne, *Anal. Chem.* **2005**, *77*, 338 A.
- [2] J. H. Granger, M. C. Granger, M. A. Firpo, S. J. Mulvihill, M. D. Porter, *Analyst* **2012**, *138*, 410.
- [3] R. A. Halvorson, P. J. Vikesland, *Environ. Sci. Technol.* **2010**, *44*, 7749.
- [4] B. de Nijs, C. Carnegie, I. Szabó, D.-B. Grys, R. Chikkaraddy, M. Kamp, S. J. Barrow, C. A. Readman, M.-E. Kleemann, O. A. Scherman, E. Rosta, J. J. Baumberg, *ACS Sens.* **2019**, *4*, 2988.
- [5] A. P. Craig, A. S. Franca, J. Irudayaraj, *Annu. Rev. Food Sci. Technol.* **2013**, *4*, 369.
- [6] T. Yang, Z. Zhang, B. Zhao, R. Hou, A. Kinchla, J. M. Clark, L. He, *Anal. Chem.* **2016**, *88*, 5243.
- [7] N. H. Ly, T. H. Nguyen, N. D. Nghi, Y.-H. Kim, S.-W. Joo, *Sensors* **2019**, *19*, 1355.
- [8] L. He, Y. Liu, M. Lin, J. Awika, D. R. Ledoux, H. Li, A. Mustapha, *Sens. Instrum. Food Qual. Saf.* **2008**, *2*, 66.
- [9] J. Zheng, L. He, *Compr. Rev. Food Sci. Food Saf.* **2014**, *13*, 317.
- [10] B. de Nijs, M. Kamp, I. Szabó, S. J. Barrow, F. Benz, G. Wu, C. Carnegie, R. Chikkaraddy, W. Wang, W. M. Deacon, E. Rosta, J. J. Baumberg, O. A. Scherman, *Faraday Discuss.* **2017**, *205*, 505.
- [11] J. H. Granger, N. E. Schlotter, A. C. Crawford, M. D. Porter, *Chem. Soc. Rev.* **2016**, *45*, 3865.
- [12] D. L. Jeanmaire, R. P. Van Duyne, *J. Electroanal. Chem. Interfacial Electrochem.* **1977**, *84*, 1.
- [13] D. Cialla, A. März, R. Böhme, F. Theil, K. Weber, M. Schmitt, J. Popp, *Anal. Bioanal. Chem.* **2012**, *403*, 27.
- [14] M. J. Banholzer, J. E. Millstone, L. Qin, C. A. Mirkin, *Chem. Soc. Rev.* **2008**, *37*, 885.
- [15] B. Sharma, R. R. Frontiera, A.-I. Henry, E. Ringe, R. P. Van Duyne, *Mater. Today* **2012**, *15*, 16.
- [16] E. C. Le Ru, P. G. Etchegoin, *Chem. Phys. Lett.* **2006**, *423*, 63.
- [17] D.-B. Grys, B. de Nijs, A. R. Salmon, J. Huang, W. Wang, W.-H. Chen, O. A. Scherman, J. J. Baumberg, *ACS Nano* **2020**, *14*, 8689.
- [18] S. E. J. Bell, G. Charron, E. Cortés, J. Kneipp, M. L. de la Chapelle, J. Langer, M. Procházka, V. Tran, S. Schlücker, *Angew. Chem., Int. Ed.* **2020**, *59*, 5454.
- [19] S. J. Barrow, S. Kasera, M. J. Rowland, J. del Barrio, O. A. Scherman, *Chem. Rev.* **2015**, *115*, 12320.
- [20] J. Turkevich, P. C. Stevenson, J. Hillier, *Discuss. Faraday Soc.* **1951**, *11*, 55.
- [21] G. Frens, *Nat. Phys. Sci.* **1973**, *241*, 20.
- [22] L. Tong, H. Xu, M. Käll, *MRS Bull.* **2014**, *39*, 163.
- [23] C. Ciraci, R. T. Hill, J. J. Mock, Y. Urzhumov, A. I. Fernández-Domínguez, S. A. Maier, J. B. Pendry, A. Chilkoti, D. R. Smith, *Science* **2012**, *337*, 1072.
- [24] C. Readman, B. de Nijs, I. Szabó, A. Demetriadou, R. Greenhalgh, C. Durkan, E. Rosta, O. A. Scherman, J. J. Baumberg, *Nano Lett.* **2019**, *19*, 2051.
- [25] R. W. Taylor, T.-C. Lee, O. A. Scherman, R. Esteban, J. Aizpurua, F. M. Huang, J. J. Baumberg, S. Mahajan, *ACS Nano* **2011**, *5*, 3878.
- [26] B. de Nijs, R. W. Bowman, L. O. Herrmann, F. Benz, S. J. Barrow, J. Mertens, D. O. Sigle, R. Chikkaraddy, A. Eiden, A. Ferrari, O. A. Scherman, J. J. Baumberg, *Faraday Discuss.* **2015**, *178*, 185.
- [27] D. O. Sigle, S. Kasera, L. O. Herrmann, A. Palma, B. de Nijs, F. Benz, S. Mahajan, J. J. Baumberg, O. A. Scherman, *J. Phys. Chem. Lett.* **2016**, *7*, 704.
- [28] L. Bi, Y. Wang, Y. Yang, Y. Li, S. Mo, Q. Zheng, L. Chen, *ACS Appl. Mater. Interfaces* **2018**, *10*, 15381.
- [29] W. Zhang, B. Li, L. Chen, Y. Wang, D. Gao, X. Ma, A. Wu, *Anal. Methods* **2014**, *6*, 2066.
- [30] Q. Su, X. Ma, J. Dong, C. Jiang, W. Qian, *ACS Appl. Mater. Interfaces* **2011**, *3*, 1873.
- [31] Q. Fu, Z. Zhan, J. Dou, X. Zheng, R. Xu, M. Wu, Y. Lei, *ACS Appl. Mater. Interfaces* **2015**, *7*, 13322.
- [32] U. S. Dinish, F. C. Yaw, A. Agarwal, M. Olivo, *Biosens. Bioelectron.* **2011**, *26*, 1987.
- [33] Q. Yang, M. Deng, H. Li, M. Li, C. Zhang, W. Shen, Y. Li, D. Guo, Y. Song, *Nanoscale* **2014**, *7*, 421.
- [34] Y. Liu, Z. Lu, X. Lin, H. Zhu, W. Hasi, M. Zhang, X. Zhao, X. Lou, *RSC Adv.* **2016**, *6*, 58387.
- [35] D. Radziuk, H. Moehwald, *Phys. Chem. Chem. Phys.* **2015**, *17*, 21072.
- [36] A. Chou, E. Jaatinen, R. Buividas, G. Seniutinas, S. Juodkazis, E. L. Izake, P. M. Fredericks, *Nanoscale* **2012**, *4*, 7419.
- [37] J. Li, H. Yan, X. Tan, Z. Lu, H. Han, *Anal. Chem.* **2019**, *91*, 3885.
- [38] W. Tang, D. B. Chase, J. F. Rabolt, *Anal. Chem.* **2013**, *85*, 10702.
- [39] M. Yang, G. Liu, H. M. Mehedi, Q. Ouyang, Q. Chen, *Anal. Chim. Acta* **2017**, *986*, 122.
- [40] M. J. Oliveira, P. Quaresma, M. Peixoto de Almeida, A. Araújo, E. Pereira, E. Fortunato, R. Martins, R. Franco, H. Águas, *Sci. Rep.* **2017**, *7*, 1.
- [41] J. Zhu, X.-H. Chen, J.-J. Li, J.-W. Zhao, *Spectrochim. Acta. A. Mol. Biomol. Spectrosc.* **2019**, *211*, 154.
- [42] R. Keir, D. Sadler, W. E. Smith, *Appl. Spectrosc.* **2002**, *56*, 551.
- [43] D. He, B. Hu, Q.-F. Yao, K. Wang, S.-H. Yu, *ACS Nano* **2009**, *3*, 3993.
- [44] Y. Qu, C. Tan, Z. Zhang, L. He, *Analyst* **2017**, *142*, 4075.
- [45] Y. Wang, K. Wang, B. Zou, T. Gao, X. Zhang, Z. Du, S. Zhou, *J. Mater. Chem. C* **2013**, *1*, 2441.
- [46] X. Liu, Y. Shao, Y. Tang, K.-F. Yao, *Sci. Rep.* **2014**, *4*, 1.
- [47] T. Wang, J. Zhou, Y. Wang, *Nanomaterials* **2018**, *8*, 331.
- [48] Y. Wang, N. Lu, W. Wang, L. Liu, L. Feng, Z. Zeng, H. Li, W. Xu, Z. Wu, W. Hu, Y. Lu, L. Chi, *Nano Res.* **2013**, *6*, 159.
- [49] B. Sun, X. Jiang, H. Wang, B. Song, Y. Zhu, H. Wang, Y. Su, Y. He, *Anal. Chem.* **2015**, *87*, 1250.
- [50] S. Jiang, J. Guo, C. Zhang, C. Li, M. Wang, Z. Li, S. Gao, P. Chen, H. Si, S. Xu, *RSC Adv.* **2017**, *7*, 5764.
- [51] W. Wang, Y. Yin, Z. Tan, J. Liu, *Nanoscale* **2014**, *6*, 9588.
- [52] N. M. B. Perney, J. J. Baumberg, M. E. Zoorob, M. D. B. Charlton, S. Mahnkopf, C. M. Netti, *Opt. Express* **2006**, *14*, 847.
- [53] B. Daglar, G. B. Demirel, T. Khudiyev, T. Dogan, O. Tobail, S. Altuntas, F. Buyukserin, M. Bayindir, *Nanoscale* **2014**, *6*, 12710.
- [54] W. Tao, A. Zhao, H. Sun, Z. Gan, M. Zhang, D. Li, H. Guo, *RSC Adv.* **2013**, *4*, 3487.
- [55] C. Muehlethaler, M. Leona, J. R. Lombardi, *Forensic Sci. Int.* **2016**, *268*, 1.

- [56] L. He, J. Huang, T. Xu, L. Chen, K. Zhang, S. Han, Y. He, S. T. Lee, *J. Mater. Chem.* **2011**, *22*, 1370.
- [57] X. Li, H. Hu, D. Li, Z. Shen, Q. Xiong, S. Li, H. J. Fan, *ACS Appl. Mater. Interfaces* **2012**, *4*, 2180.
- [58] Y. Zhu, M. Li, D. Yu, L. Yang, *Talanta* **2014**, *128*, 117.
- [59] L. Yang, Y. Peng, Y. Yang, J. Liu, H. Huang, B. Yu, J. Zhao, Y. Lu, Z. Huang, Z. Li, J. R. Lombardi, *Adv. Sci.* **2019**, *6*, 1900310.
- [60] Z. Liu, L. Cheng, L. Zhang, C. Jing, X. Shi, Z. Yang, Y. Long, J. Fang, *Nanoscale* **2014**, *6*, 2567.
- [61] M. Kahl, E. Voges, S. Kostrewa, C. Viets, W. Hill, *Sens. Actuators B Chem.* **1998**, *51*, 285.
- [62] B. Li, W. Zhang, L. Chen, B. Lin, *Electrophoresis* **2013**, *34*, 2162.
- [63] R. Que, M. Shao, S. Zhuo, C. Wen, S. Wang, S.-T. Lee, *Adv. Funct. Mater.* **2011**, *21*, 3337.
- [64] A. Y. F. Mahmoud, C. J. Rusin, M. T. McDermott, *Analyst* **2020**, *145*, 1396.
- [65] M. Fan, A. G. Brolo, *Phys. Chem. Chem. Phys.* **2009**, *11*, 7381.
- [66] N. Michieli, R. Pilot, V. Russo, C. Scian, F. Todescato, R. Signorini, S. Agnoli, T. Cesca, R. Bozio, G. Mattei, *RSC Adv.* **2017**, *7*, 369.

**How to cite this article:** Grys D-B, Chikkaraddy R, Kamp M, Scherman OA, Baumberg JJ, de Nijs B. Eliminating irreproducibility in SERS substrates. *J Raman Spectrosc.* 2021;52:412–419. <https://doi.org/10.1002/jrs.6008>